Hindawi
Advances in Materials Science and Engineering
Volume 2017, Article ID 7121785, 9 pages
https://doi.org/10.1155/2017/7121785

Research Article

Thermal Effect on Structural Interaction between Energy Pile and Its Host Soil

Qingwen Li,[1,2] Lu Chen,[1] and Lan Qiao[1]

[1]*Department of Civil Engineering, University of Science and Technology Beijing, Beijing 100083, China*
[2]*State Key Laboratory of Building Safety and Built Environment, China Academy of Building Research, Beijing 100013, China*

Correspondence should be addressed to Qingwen Li; qingwenli@ustb.edu.cn

Received 6 April 2017; Revised 23 June 2017; Accepted 4 July 2017; Published 15 August 2017

Academic Editor: Shuo Yin

Energy pile is one of the promising areas in the burgeoning green power technology; it is gradually gaining attention and will have wide applications in the future. Because of its specific structure, the energy pile has the functions of both a structural element and a heat exchanger. However, most researchers have been paying attention to only the heat transfer process and its efficiency. Very few studies have been done on the structural interaction between the energy pile and its host soil. As the behavior of the host soil is complicated and uncertain, thermal stresses appear with inhomogeneous distribution along the pile, and the peak value and distribution of stress will be affected by the thermal and physical properties and thermal conductivities of the structure and the host soil. In view of the above, it is important to determine thermal-mechanical coupled behavior under these conditions. In this study, a comprehensive method using theoretical derivations and numerical simulation was adopted to analyze the structural interaction between the energy pile and its host soil. The results of this study could provide technical guidance for the construction of energy piles.

1. Introduction

In the 1980s, geotechnical engineers in Austria and Switzerland began to use the building foundation as a heat exchanger for the ground-source heat pump (GSHP). The GSHP is a device that can better utilize the energy stored in the soil to transfer the stored heat energy to the structure using pipes laid underground and realize energy balance during both winter and summer. In summer, the host soil acts as a heat sink by transferring the heat from the buildings into the host soil. In winter, the host soil acts as a heat source and transports the heat from the host soil to the buildings. Energy pile is one of the promising areas in the burgeoning green power technology; it is gradually gaining attention and will have wide applications in the future. By taking advantage of the good thermal conductivity of concrete in the energy pile and the large heat exchange area between the pile and the host soil, the performance of the heat exchanger could be improved. Moreover, the energy pile can save the cost of drilling holes and preserve the underground space resources. Compared to the conventional GSHP that has been in use in the past 20 years, the energy pile system (bored pile, precast concrete pile, and underground diaphragm wall) has witnessed rapid development globally, especially in Canada, Japan, and some European countries.

Because of its specific structure, the energy pile has the functions of both a structural element and a heat exchanger. It must withstand not only forces such as the frictional force and tip resistance, and the stresses as in the case of normal piles, but also the thermal stresses caused by the temperature changes during heat transfer. However, most researchers have been paying attention only to the heat transfer process and efficiency. In connection with heat transfer in an energy pile, Gao et al. (2008) studied the thermal performance and ground temperature of vertical pile-foundation heat exchangers and aimed at providing guidelines for improving the design of large-scale ground-coupled heat pumps in a district heating and cooling system [1]; Moon and Choi (2015) studied the heating performance characteristics of a GSHP system with energy piles and energy slabs [2]; Faizal et al. (2016) analyzed the heat transfer enhancement mechanism of geothermal energy piles [3]; Caulk et al. (2016) reported

the parameterization of a calibrated geothermal energy pile model [4]; Ghasemi-Fare and Basu (2016) presented a predictive assessment of heat exchange performance of geothermal piles [5]. Regarding studies on laying of piles, Cui et al. (2011) analyzed the heat transfer performance of pile geothermal heat exchangers with spiral coils [6]; Go et al. (2014) designed an energy pile with a spiral coil by considering the effective thermal resistance of the borehole and the effects of groundwater advection [7]; Xiang et al. (2015) developed a new practical numerical model for the energy pile with spiral coils [8]; Fadejev and Kurnitski (2015) used a whole building simulation software to simulate the geothermal energy piles and borehole design with heat pump [9]; Park et al. (2015) studied the coil-type ground heat exchanger by considering the relative constructability and thermal performance of a cast-in-place concrete energy pile [10]; Park et al. (2016) calculated the influence of coil pitch on the thermal performance of coil-type cast-in-place energy piles [11]; Yang et al. (2016) conducted laboratory investigations to analyze the thermal performance of an energy pile with spiral coil ground heat exchanger [12]. Several scholars had conducted research on the heat exchange efficiency of energy piles. Bozis et al. (2011) evaluated the effects of design parameters on the efficiency of heat transfer in energy piles [13]; Park et al. (2015) estimated the constructability and heat exchange efficiency of large diameter cast-in-place energy piles with various configurations of heat exchange pipes [14]; Yoon et al. (2015) reported the thermal efficiency and cost analysis of different types of ground heat exchangers in energy piles [15]; Cecinato and Loveridge (2015) analyzed the factors influencing the thermal efficiency of energy piles [16]; Astrain et al. (2016) performed a comparative study of different heat exchanger systems in a thermoelectric refrigerator and their influence on efficiency [17]; Akrouch et al. (2016) conducted experimental, analytical, and numerical studies on the thermal efficiency of energy piles in unsaturated soils [18]. On energy piles, there are some more research papers which provide technical guidelines for the construction of heat exchanger [19–21].

Numerical simulation is an important prediction method in engineering because of its high accuracy and low cost and the rapid development of computer techniques. Hence, many scholars use analytical tools such as finite element analysis software and finite difference software to solve problems on energy piles. Bezyan et al. (2015) built a 3D model to simulate the heat transfer in geothermal pile-foundation heat exchangers with a spiral pipe configuration [22]; Pu et al. (2015) developed a new practical numerical model for the energy pile with vertical U-tube heat exchangers [23]. Further, several scholars had conducted research on energy piles using numerical simulation methods [24–26]. Most of the above research work covers theoretical analysis, laying of piles, heat exchange efficiency, field test, and numerical simulation of energy piles. However, studies on the structural interaction between the energy pile and its host soil are scarce. As the behavior of the host soil is complicated and uncertain, thermal stresses appear with inhomogeneous distribution along the pile, and the peak value and distribution of stress would be influenced by the thermal and physical properties and thermal conductivities of the structure and the host soil. In view of the above, it is important to determine the thermal-mechanical coupled behavior under these conditions. In this study, a comprehensive method using theoretical derivations and numerical simulation was adopted to analyze the structural response between the energy pile and its host soil. The results of this study can provide technical guidance for the construction of energy piles engineering.

2. Theoretical Analysis

As the foundation of the structure, the energy pile should be able to withstand forces such as the frictional force and tip resistance and the stresses as in the case of normal piles. The lateral friction force of the energy pile can be calculated by the β method.

$$q_l = \sigma_v k tg\beta, \tag{1}$$

where $\beta = ktg\phi$, k is the soil pressure coefficient, ϕ is internal friction angle, and σ_v is the vertical effective stress.

The tip resistance force can be obtained using the rigid-plastic body theory; the tip resistance force is given by

$$q_t = CN_c + \frac{1}{2}\gamma_1 BN_r + \gamma h N_q, \tag{2}$$

where N_c is the effect factor of cohesion, N_r is the loading factor for the weight of the soil, N_q is the overload factor, B is the diameter of the tip of the pile, h is the depth of the buried soil, γ_1 is the specific gravity of the soil, and γ is the average specific gravity of the soil.

The thermal stress due to temperature variations resulting from heat transfer should be considered. According to Fourier's law, the equation for heat conduction could be expressed as

$$\frac{\partial T}{\partial t} = \frac{1}{C_p \rho}\left(k_x \frac{\partial^2 T}{\partial x^2} + k_y \frac{\partial^2 T}{\partial y^2}\right), \tag{3}$$

where T is the temperature, C_p is the specific heat, and ρ is the density; k_x and k_y are the thermal conductivities in the x- and y-directions, respectively.

For deformable materials, the stress increment caused by a change in temperature is given by

$$\Delta\sigma_{ij} = -\delta_{ij} K \alpha^T \Delta T, \tag{4}$$

where $\Delta\sigma_{ij}$ is the stress increment. δ_{ij} is the Kronecker delta; when $i = j$, its value is 1, and when $i \neq j$, its value is 0; K is the bulk modulus, α^T is the coefficient of thermal expansion, and ΔT is the temperature increment.

According to the generalized Hooke's law,

$$\sigma_{ij} = 2G\varepsilon_{ij} + 3\lambda\varepsilon_{kk}\delta_{ij}, \tag{5}$$

where σ_{ij} is the stress, ε_{ij} is the total strain, ε_{kk} is the normal strain, $\lambda = E\nu/(1+\nu)(1-2\nu)$, and $G = E/2(1+\nu)$.

Lewis and Schrefler (1987) proposed the effective stress σ_{ij} [27] caused by change in temperature as follows.

$$\sigma_{ij} = 2G\left(\varepsilon_{ij} + \delta_{ij}\frac{\nu}{1-2\nu}\varepsilon_{kk}\right) - K\alpha^T \Delta T \delta_{ij}. \tag{6}$$

Table 1: Parameters of different layers of soil.

Layers	Density (kg/m^3)	Parameters			
		Bulk (Pa)	Shear (Pa)	Cohesion (Pa)	Friction angle (°)
Silty clay 1	1630	6.349×10^6	3.101×10^6	14.3	23.2
Silty-fine sand	1750	6.818×10^6	3.516×10^6	0	25.4
Silty clay 2	1740	6.944×10^6	3.968×10^6	17.6	20.6
Silty clay 3	1720	7.639×10^6	4.365×10^6	13.7	24.4
Floury soil	1750	8.472×10^6	5.984×10^6	11.4	26.3
Fine sand 1	1860	20.556×10^6	6.175×10^6	0	17.8
Fine sand 2	1820	20.556×10^6	6.175×10^6	0	17.8
Silty clay 4	1780	25.510×10^6	9.398×10^6	26.5	27.1

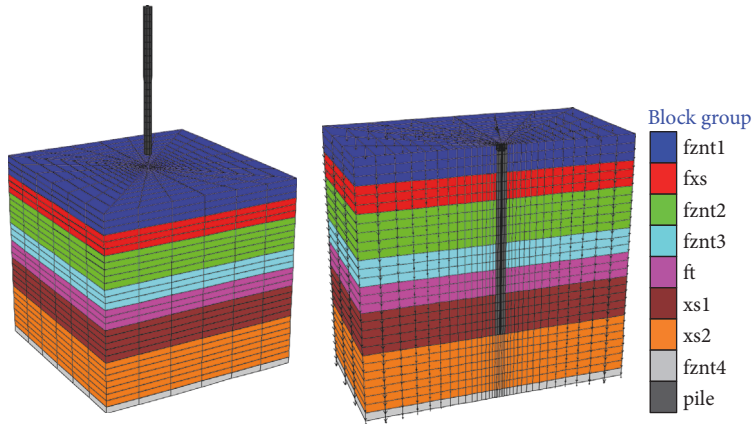

Figure 1: Simulation model of energy pile.

3. Numerical Simulation of Normal Pile

3.1. Simulation Model and Parameters. To predict the structural response between the energy pile and its host soil, a 3D model was built in finite difference software FLAC3D, as shown in Figure 1.

In the model, the physical element was used to build the pile and host soil, and the "*interface*" command was adopted to simulate the contact surfaces between the pile and the host soil. The length of the pile is 11 m along the Z-direction. The pile has a radius of 0.3 m. The host soil zone has a length of 16 m, X (−8 m, 8 m), a width of 16 m, Y (−8 m, 8 m), and a height of 15 m, Z (−15 m, 0 m); it was divided into eight layers of soil with different thicknesses. The pile was represented as an isotropic elastic model with the parameters of C30 concrete, having an elasticity modulus of 30 GPa and Poisson's ratio of 0.2. The parameters of the soil layers are presented in Table 1.

3.2. Simulation of Pile. To obtain accurate results of simulation, 12 monitoring points (0 m, 1 m, 2 m, 3 m, 4 m, 5 m, 6 m, 7 m, 8 m, 9 m, 10 m, and 11 m) were set to monitor the lateral friction stress, axial stress, and tip resistance stress under different loads (55 kN, 110 kN, 165 kN, 220 kN, 275 kN, 330 kN, 385 kN, 440 kN, 495 kN, 550 kN, 690 kN, 825 kN, 960 kN, 1100 kN, and 1375 kN). A typical contour of the lateral stresses under a load of 385 kN, obtained from simulation results, is shown in Figure 2.

Based on the results obtained under different loads, the graphs for lateral stress versus depth are plotted as shown in Figure 3.

From Figure 3, it can be seen that the lateral friction stresses change at the interface of different layers, which indicates that the lateral friction stresses are affected by the soil properties; they tend to increase toward the end of the pile and have the largest value at the end of the pile. For different loads, the curves follow the same trend; the larger the loads, the larger the lateral friction force.

A typical contour of the axial stress under a load of 385 kN is shown in Figure 4, based on the results of numerical analysis. The variation in axial stress along the depth under different loads is shown in Figure 5.

With increase in depth, the axial stresses decrease; the rate of decrease is gradual at the top of the pile, but the rate increases as the depth increases. Moreover, under different covered loading, a larger load causes a higher axial stress.

3.3. Analysis of Mechanical Characteristics of the Pile. The tip resistance stress and lateral friction stress are the important parameters in the analysis of mechanical characteristics of the pile. From the predicted results of simulation, the variation in total stress and the percentages of tip resistance and lateral

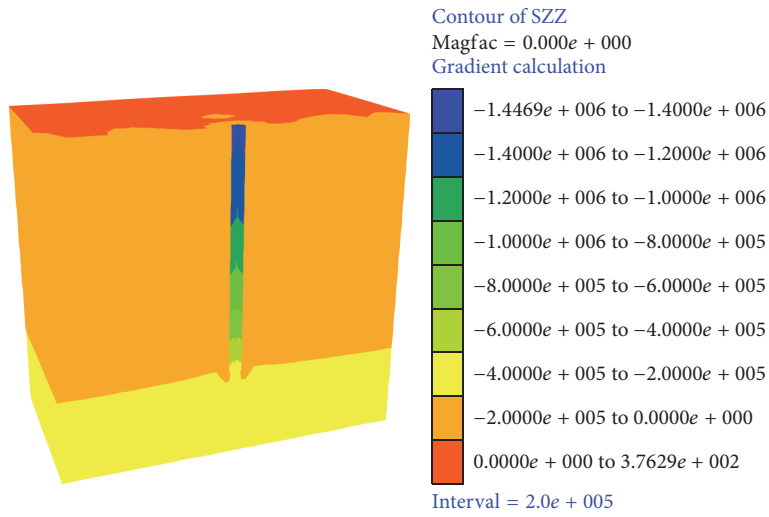

Figure 2: Typical contour of lateral stress under a load of 385 kN.

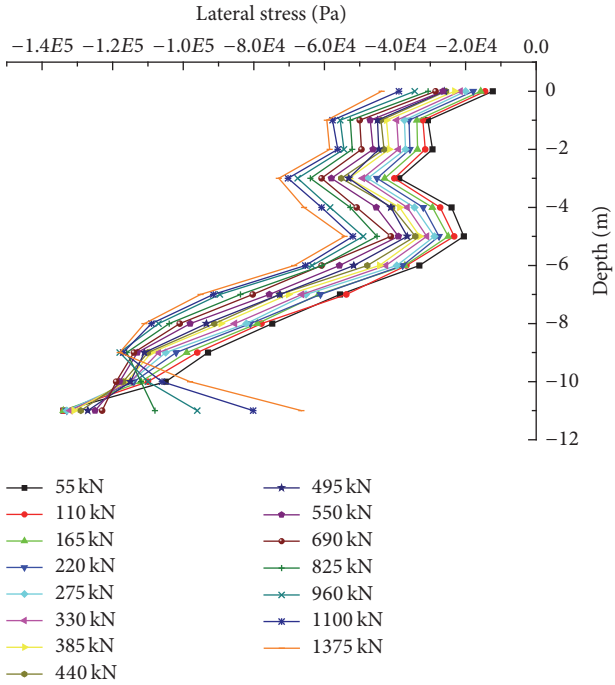

Figure 3: Variation in lateral stress along the depth of the pile.

friction stresses were calculated; these are shown in Figures 6 and 7, respectively.

From these figures, it can be seen that both the tip resistance stress and lateral friction stress vary with different loads. A larger load leads to a larger proportion of tip resistance stress and a lower proportion of lateral friction stress. Under smaller loading levels (less than 495 kN), the loads are mainly taken up by the lateral friction stress; most of the load is resisted in the host soil by the lateral friction effect, and the tip resistance stresses play a small role. With the increase in covered loads, the lateral stress increases. After the covered load exceeds 690 kN, the increase in load is taken up by the tip resistance stress; the major load-bearing role is gradually taken by the tip resistance stress, and the proportion of tip resistance stress increases.

3.4. Pile Stability Analysis. The load-displacement curve is a direct representation of the stability of the pile. From the simulation results, the load-displacement curve for the pile is plotted, as shown in Figure 8.

According to the technical code for building pile foundation, for buildings with height less than 100 m, the allowable displacement is 350 mm; for buildings with heights in the range of 100–200 m, the allowable value of settling is 250 mm; and for buildings with heights greater than 200 m, the allowable value of settling is 150 mm. Thus, to ensure absolute safety, 150 mm was chosen in this study as the allowable value of settling. As shown in Figure 8, there is a significant increase in tip displacement with increase in covered loading. At loads greater than 825 kN, the displacement of the pile increases sharply. When the covered loading increases to 1100 kN, the settling value exceeds 180 mm, which would affect the safety of the structures. Hence, in real engineering structures, if the load is greater than 875 kN, the length or the quantity of piles should be revised to improve the bearing capacity.

4. Numerical Simulation of Energy Pile under Thermal Effect

4.1. Superficial Soil Temperature and Working Temperature. In Beijing area, the ground surface temperature is approximately −5°C in winter, and it reaches 28.5°C in summer. The temperature of the host soil would become stable with increase in depth. The variations in superficial soil temperature with depth in winter and summer are shown in Figure 9.

According to the stipulations in "Technical Code for Ground-Source Heat Pump System, 2009, China [28]," in summer, the working temperature at the water outlet of the heat exchanger pipe should not exceed 33°C, and the working temperature at the water inlet of the heat exchanger

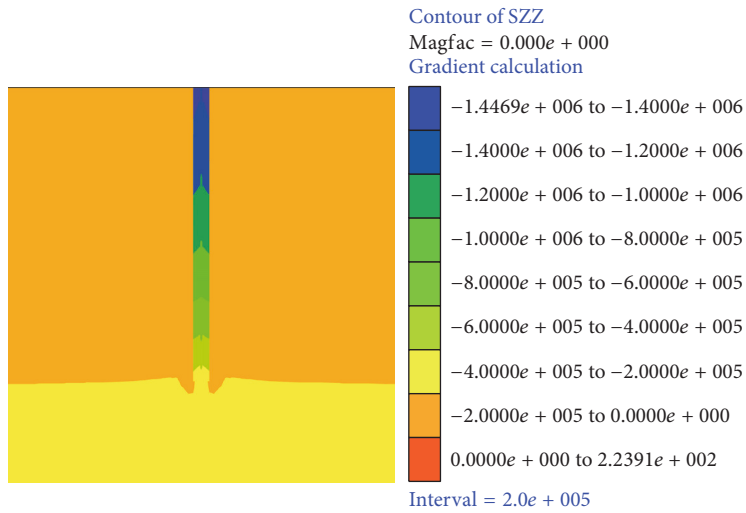

Figure 4: Typical contour of axial stress under a load of 385 kN.

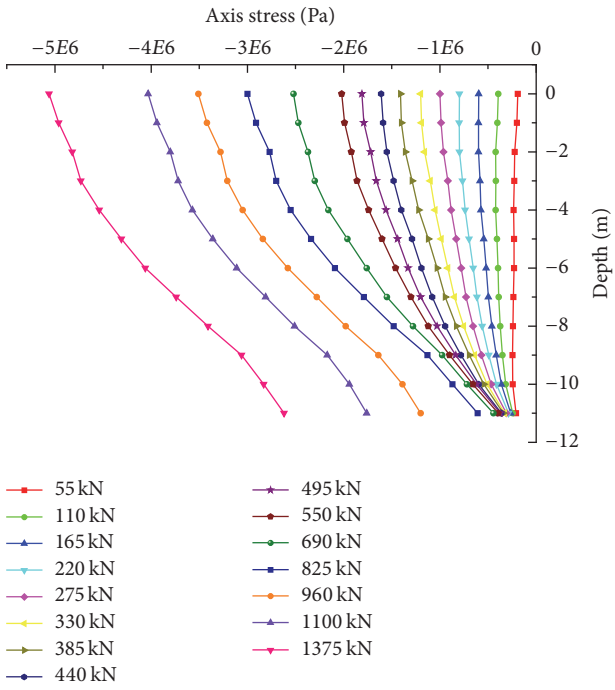

Figure 5: Variation in axial stress along the depth of the pile.

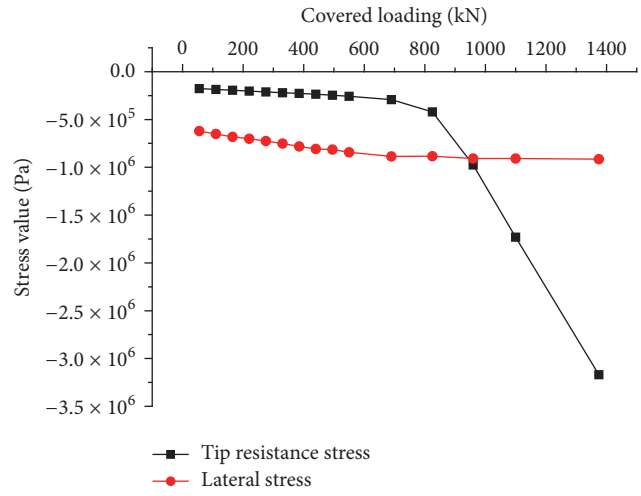

Figure 6: Total stress under different loads.

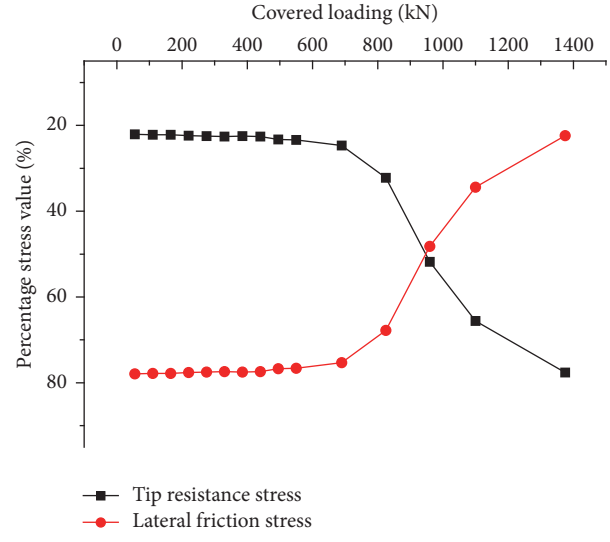

Figure 7: Share of stresses under different loads.

pipe should be more than 4°C. In this numerical simulation, to estimate the worst-case scenario for the stability of the energy pile, the two extreme temperatures (33°C and 4°C) were assumed as the working temperatures in summer and in winter, respectively.

4.2. Simulation Parameters and Boundary Conditions. Recent studies on energy piles show that spiral coil with the largest heat exchange surface of the fluid pipe is the optimal type of heat exchanger for a cast-in-place energy pile. From the results of thermal efficiency analysis, it is found that the spiral coil type has the best heating and cooling performance, with

Table 2: Thermal parameters of different layers of host soil and concrete.

	Thermal expansivity (1/K)	Thermal conductivity coefficient, X-direction (W/m/K)	Thermal conductivity coefficient, Y-direction (W/m/K)
Silty clay 1	$1.8e^{-5}$	1.36	1.28
Silty clay 2	$1.8e^{-5}$	1.36	1.28
Floury soil	$1.5e^{-5}$	1.14	1.06
Fine sand 2	$2.1e^{-5}$	0.98	1.02
Silty-fine sand	$2.3e^{-5}$	1.19	1.13
Silty clay 3	$1.8e^{-5}$	1.36	1.28
Fine sand 1	$2.1e^{-5}$	0.98	1.02
Silty clay 4	$2.2e^{-5}$	1.46	1.45
Concrete	$1.2e^{-5}$	1.28	1.28

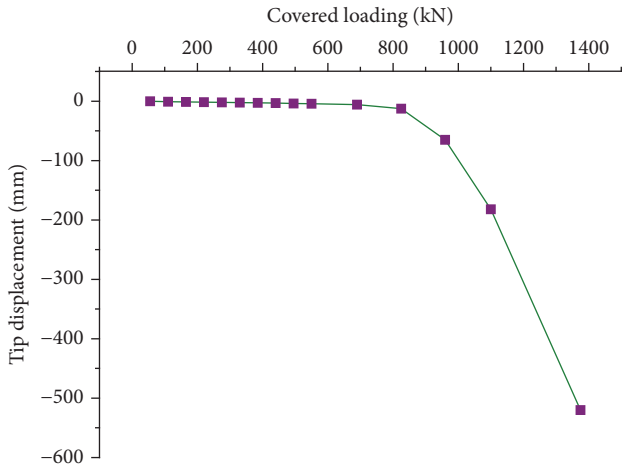

Figure 8: Load-displacement curve under different covered loading.

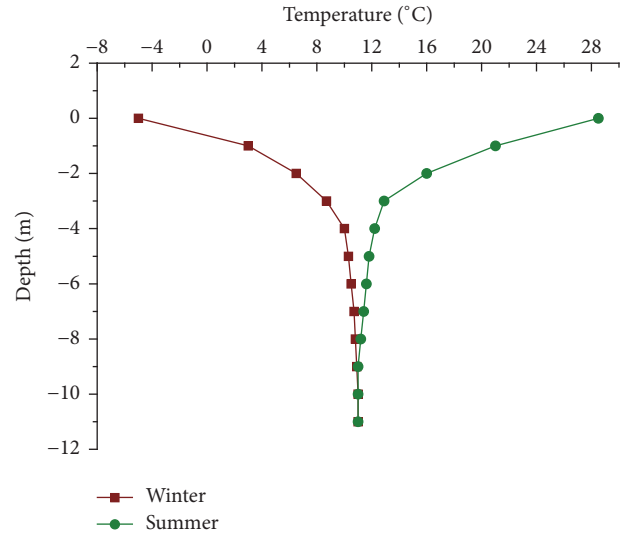

Figure 9: Variation in temperature with depth.

thermal efficiency nearly 150% of that of the double-U type [29]. A typical spiral coil heat exchanger cast-in-place energy pile and its detailed dimensions are shown in Figure 10. Based on the above results, in this simulation, a heat exchanger with spiral coil was selected; to simplify the modeling process and apply appropriate temperature boundary conditions, the spiral coil heat exchanger system can be equivalent to the form of a cylinder with 0.5 m external diameter which was selected. A working temperature of 33°C was assigned to the equivalent pipe in summer, and a working temperature of 4°C was assigned to the equivalent pipe in winter. The boundary conditions for temperature in the different layers of the soil, shown in Figure 9, were applied for the simulation.

In the simulation, nonhomogeneous thermal conductivities of the soil were applied by considering the effect of different levels of compaction, uneven layers, and other soil properties. The thermal parameters of the specimens obtained by cutting rings from different positions were tested using a DRE-III heat conductivity coefficient tester. The measuring probe and the testing instrument are shown in Figure 11.

The test results of the thermal parameters of different layers of the host soil and concrete are presented in Table 2.

4.3. Analysis of Simulation Results. In FLAC3D software, the pore pressure command was used to analyze the heat diffusion in the energy pile. From the simulation results, the typical thermal diffusion contour was obtained; this is shown in Figure 12.

During the simulation, the monitoring points were set at intervals of 1 m for reading the output. From the simulation results, the curves for the predicted temperature and its variation on the energy pile surface in winter and summer were obtained; the curves corresponding to winter and summer are shown in Figures 13(a) and 13(b), respectively.

Based on the simulation results, the thermal stresses were estimated. Further, the percentage share of the lateral friction stress and tip resistance stress under different covered loading in winter and summer was estimated; the corresponding values in the case of a normal pile were also estimated. These results are shown in Figure 14.

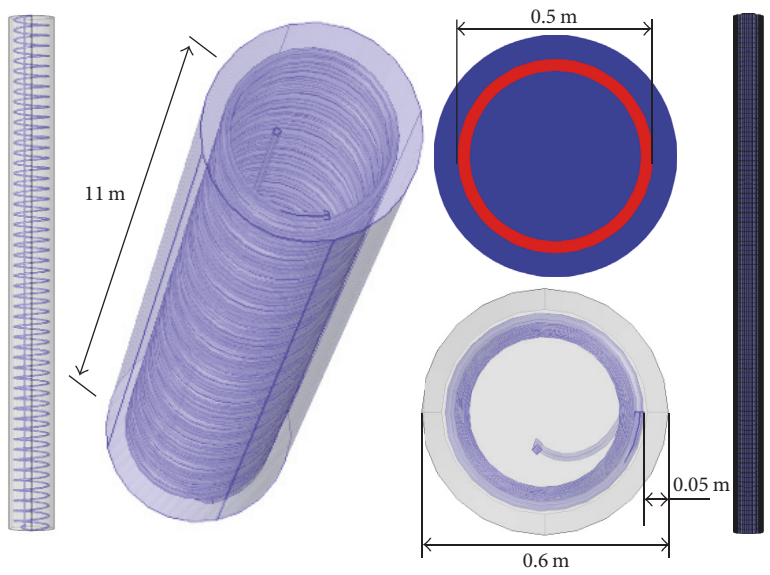

Figure 10: Conceptual model and simulation model of energy pile.

Figure 11: DRE-III heat conductivity coefficient tester and measuring probe.

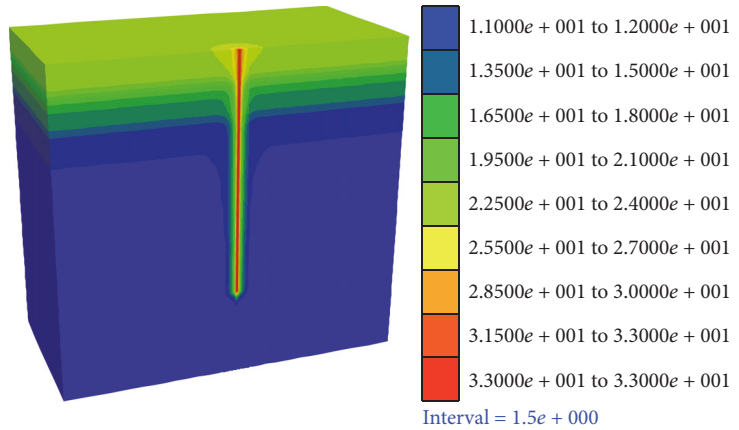

Figure 12: Thermal diffusion contour of energy pile in summer.

As shown in Figure 14, the lateral friction stress increases with load in summer; this provides some advantage in maintaining the stability of the energy pile. However, in winter, because of the effect of low temperature, the proportion of lateral friction stress in the total stress decreases with load; this will have an adverse effect in maintaining the stability of the energy pile.

5. Discussion and Conclusion

In this paper, using finite difference simulation, a series of predicted results on the structural interaction between the energy pile and its host soil are presented.

(1) The lateral friction stress changes at the interface of different layers, which indicates that the lateral friction force is affected by the soil properties; it tends to increase toward

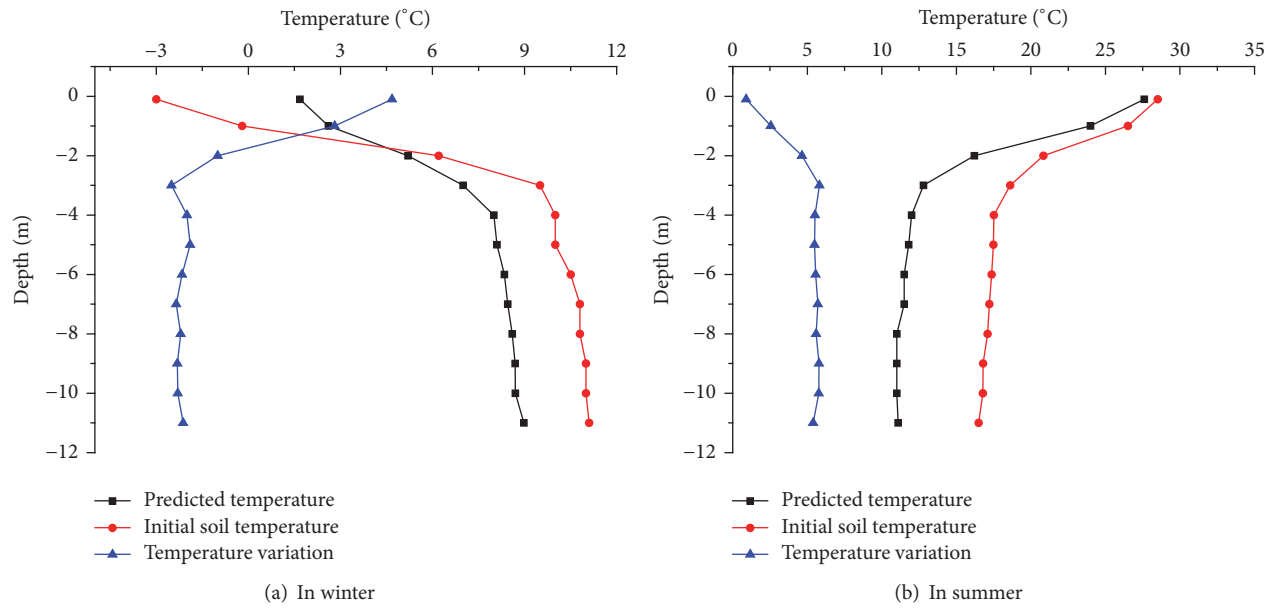

Figure 13: Predicted temperature and its variation on energy pile surface.

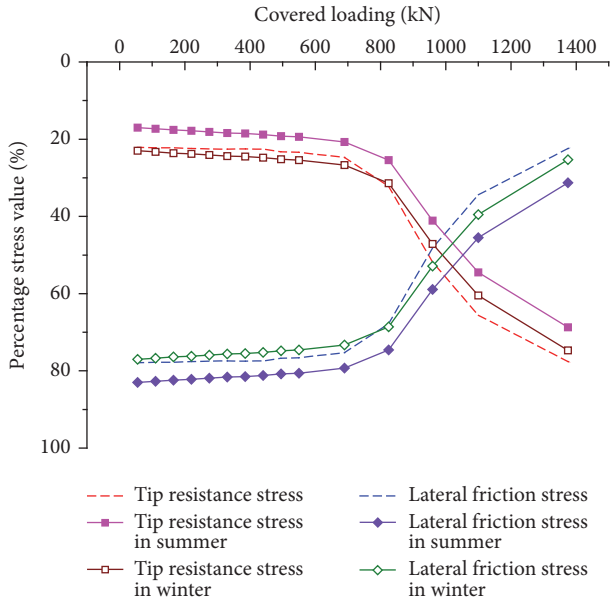

Figure 14: Percentage stress value under different covered loading in winter and summer.

the end of the pile and has the largest value at the end of the pile. For different loads, the curves follow the same trend; the larger the covered loading, the larger the lateral friction stress.

(2) Both the tip resistance stress and lateral friction stress are different under different covered loading. A larger load leads to a larger proportion of tip resistance stress and a lower proportion of lateral friction stress. Under smaller loading levels, the load is mainly taken up by the lateral friction stress; a large proportion of the load is resisted in the host soil by the lateral friction effect, and the tip resistance stress plays a small role. With the increase in covered loading, the lateral stress increases. After the covered loading exceeds 690 kN, the increase in load is taken up by the tip resistance stress; the major load-bearing role is gradually taken by the tip resistance stress, and the proportion of tip resistance stress increases.

(3) There is a significant increase in tip displacement with increase in covered loading. At loads greater than 825 kN, the displacement of the pile increases sharply. When the covered loading increases to 1100 kN, the settling value exceeds 180 mm, which would affect the safety of the structure. Hence, in real engineering structures, if the covered loading is greater than 875 kN, the length or the quantity of the pile should be revised to improve bearing capacity.

(4) In summer, the lateral friction stress increases with load; this provides some advantage in maintaining the stability of the energy pile. However, in winter, because of the effect of low temperature, the proportion of lateral friction stress in the total stress decreases with load; this will have an adverse effect in maintaining the stability of the energy pile. Hence, it is necessary to provide more supporting capacity to ensure the stability of the energy pile.

Conflicts of Interest

The authors declare that they have no conflicts of interest.

Acknowledgments

This work was supported by the Opening Funds of State Key Laboratory of Building Safety and Built Environment (no. BSBE2015-06) and Joint Research Program between University of Science and Technology Beijing and National Taipei University of Technology (no. TW201703).

References

[1] J. Gao, X. Zhang, J. Liu, K. S. Li, and J. Yang, "Thermal performance and ground temperature of vertical pile-foundation heat exchangers: a case study," *Applied Thermal Engineering*, vol. 28, no. 17-18, pp. 2295–2304, 2008.

[2] C.-E. Moon and J. M. Choi, "Heating performance characteristics of the ground source heat pump system with energy-piles and energy-slabs," *Energy*, vol. 81, pp. 27–32, 2015.

[3] M. Faizal, A. Bouazza, and R. M. Singh, "Heat transfer enhancement of geothermal energy piles," *Renewable and Sustainable Energy Reviews*, vol. 57, pp. 16–33, 2016.

[4] R. Caulk, E. Ghazanfari, and J. S. McCartney, "Parameterization of a calibrated geothermal energy pile model," *Geomechanics for Energy and the Environment*, vol. 5, pp. 1–15, 2016.

[5] O. Ghasemi-Fare and P. Basu, "Predictive assessment of heat exchange performance of geothermal piles," *Renewable Energy*, vol. 86, pp. 1178–1196, 2016.

[6] P. Cui, X. Li, Y. Man, and Z. Fang, "Heat transfer analysis of pile geothermal heat exchangers with spiral coils," *Applied Energy*, vol. 88, no. 11, pp. 4113–4119, 2011.

[7] G.-H. Go, S.-R. Lee, S. Yoon, and H.-B. Kang, "Design of spiral coil PHC energy pile considering effective borehole thermal resistance and groundwater advection effects," *Applied Energy*, vol. 125, pp. 165–178, 2014.

[8] Y. Xiang, H. Su, W. Gou et al., "A new practical numerical model for the energy pile with spiral coils," *International Journal of Heat and Mass Transfer*, vol. 91, pp. 777–784, 2015.

[9] J. Fadejev and J. Kurnitski, "Geothermal energy piles and boreholes design with heat pump in a whole building simulation software," *Energy and Buildings*, vol. 106, pp. 23–34, 2015.

[10] S. Park, D. Lee, H.-J. Choi, K. Jung, and H. Choi, "Relative constructability and thermal performance of cast-in-place concrete energy pile: Coil-type GHEX (ground heat exchanger)," *Energy*, vol. 81, pp. 56–66, 2015.

[11] S. Park, S. Lee, D. Lee, S. S. Lee, and H. Choi, "Influence of coil pitch on thermal performance of coil-type cast-in-place energy piles," *Energy and Buildings*, vol. 129, pp. 344–356, 2016.

[12] W. Yang, P. Lu, and Y. Chen, "Laboratory investigations of the thermal performance of an energy pile with spiral coil ground heat exchanger," *Energy and Buildings*, vol. 128, pp. 491–502, 2016.

[13] D. Bozis, K. Papakostas, and N. Kyriakis, "On the evaluation of design parameters effects on the heat transfer efficiency of energy piles," *Energy and Buildings*, vol. 43, no. 4, pp. 1020–1029, 2011.

[14] S. Park, C. Sung, K. Jung, B. Sohn, A. Chauchois, and H. Choi, "Constructability and heat exchange efficiency of large diameter cast-in-place energy piles with various configurations of heat exchange pipe," *Applied Thermal Engineering*, vol. 90, pp. 1061–1071, 2015.

[15] S. Yoon, S.-R. Lee, J. Xue, K. Zosseder, G.-H. Go, and H. Park, "Evaluation of the thermal efficiency and a cost analysis of different types of ground heat exchangers in energy piles," *Energy Conversion and Management*, vol. 105, pp. 393–402, 2015.

[16] F. Cecinato and F. A. Loveridge, "Influences on the thermal efficiency of energy piles," *Energy*, vol. 82, pp. 1021–1033, 2015.

[17] D. Astrain, P. Aranguren, A. Martínez, A. Rodríguez, and M. G. Pérez, "A comparative study of different heat exchange systems in a thermoelectric refrigerator and their influence on the efficiency," *Applied Thermal Engineering*, vol. 103, pp. 1289–1298, 2016.

[18] G. A. Akrouch, M. Sánchez, and J.-L. Briaud, "An experimental, analytical and numerical study on the thermal efficiency of energy piles in unsaturated soils," *Computers and Geotechnics*, vol. 71, pp. 207–220, 2016.

[19] Y. Hamada, H. Saitoh, M. Nakamura, H. Kubota, and K. Ochifuji, "Field performance of an energy pile system for space heating," *Energy and Buildings*, vol. 39, no. 5, pp. 517–524, 2007.

[20] O. Ghasemi-Fare and P. Basu, "A practical heat transfer model for geothermal piles," *Energy and Buildings*, vol. 66, pp. 470–479, 2013.

[21] H. Park, S.-R. Lee, S. Yoon, and J.-C. Choi, "Evaluation of thermal response and performance of PHC energy pile: field experiments and numerical simulation," *Applied Energy*, vol. 103, pp. 12–24, 2013.

[22] B. Bezyan, S. Porkhial, and A. A. Mehrizi, "3-D simulation of heat transfer rate in geothermal pile-foundation heat exchangers with spiral pipe configuration," *Applied Thermal Engineering*, vol. 87, pp. 655–668, 2015.

[23] L. Pu, D. Qi, K. Li, H. Tan, and Y. Li, "Simulation study on the thermal performance of vertical U-tube heat exchangers for ground source heat pump system," *Applied Thermal Engineering*, vol. 79, pp. 202–213, 2015.

[24] A. A. Mehrizi, S. Porkhial, B. Bezyan, and H. Lotfizadeh, "Energy pile foundation simulation for different configurations of ground source heat exchanger," *International Communications in Heat and Mass Transfer*, vol. 70, pp. 105–114, 2016.

[25] S. Chen, J. Mao, and X. Han, "Heat transfer analysis of a vertical ground heat exchanger using numerical simulation and multiple regression model," *Energy and Buildings*, vol. 129, pp. 81–91, 2016.

[26] Z. Han, X. Ju, X. Ma, Y. Zhang, and M. Lin, "Simulation of the performance of a hybrid ground-coupled heat pump system on the basis of wet bulb temperature control," *Applied Thermal Engineering*, vol. 108, pp. 980–988, 2016.

[27] R. W. Lewis and B. A. Schrefler, *The Finite Element Method in Deformation and Consolidation of Porous Media*, Wiley, New York, NY, USA, 1987.

[28] PRC, "M.o.H.a.U.-R.D.o.t., Technical code for ground-source heat pump system," China building industry press, 2009.

[29] J. Luo, H. Zhao, S. Gui, W. Xiang, J. Rohn, and P. Blum, "Thermo-economic analysis of four different types of ground heat exchangers in energy piles," *Applied Thermal Engineering*, vol. 108, pp. 11–19, 2016.